

# Urban meteorological modeling using WRF: a sensitivity study

Ashish Sharma,<sup>a,b\*</sup> Harindra J.S. Fernando,<sup>b</sup> Alan F. Hamlet,<sup>a,b</sup> Jessica J. Hellmann,<sup>c,d</sup>  
 Michael Barlage<sup>e</sup> and Fei Chen<sup>e</sup>

<sup>a</sup> Environmental Change Initiative (ECI), University of Notre Dame, IN, USA

<sup>b</sup> Department of Civil & Environmental Engineering and Earth Sciences (CEEES), University of Notre Dame, IN, USA

<sup>c</sup> Department of Biological Sciences, University of Notre Dame, IN, USA

<sup>d</sup> Present address: Institute on the Environment, University of Minnesota, St Paul, MN, USA

<sup>e</sup> Research Applications Laboratory, National Center for Atmospheric Research, Boulder, CO, USA

**ABSTRACT:** This study explores the sensitivity of high-resolution mesoscale simulations of urban heat island (UHI) in the Chicago metropolitan area (CMA) and its environs to urban physical parameterizations, with emphasis on the role of lake breeze. A series of climate downscaling experiments were conducted using the urban-Weather Research and Forecasting (uWRF) model at 1-km horizontal resolution for a relatively warm period with a strong lake breeze. The study employed best available morphological data sets, selection of appropriate urban parameters, and estimates of anthropogenic heating sources for the CMA. Several urban parameterization schemes were then evaluated using these parameter values. The study also examined (1) the impacts of land data assimilation for initialization of the mesoscale model, (2) the role of urbanization on UHI and lake breeze, and (3) the effects of sub-grid scale land-cover variability on urban meteorological predictions. Comparisons of temperature and wind simulations with station observations and Moderate Resolution Imaging Spectroradiometer satellite data in the CMA showed that uWRF, with appropriate selection of urban parameter values, was able to reproduce the measured near-surface temperature and wind speeds reasonably well. In particular, the model was able to capture the observed spatial variation of 2-m near-surface temperatures at night, when the UHI effect was pronounced. Results showed that inclusion of sub-grid scale variability of land-use and initializing models with more accurate land surface data can yield improved simulations of near-surface temperatures and wind speeds, particularly in the context of simulating the extent and spatial heterogeneity of UHI effects.

**KEY WORDS** urban heat island; lake breeze; urban meteorology; mesoscale modeling; land data assimilation; sub-grid scale land-use variability; WRF

Received 8 December 2015; Revised 5 May 2016; Accepted 5 June 2016

## 1. Introduction

Urban heat island (UHI) effects, defined as elevated local temperatures in urban areas compared to rural areas, are common in developed areas, and are not observed solely in strongly urbanized environments. Suburban areas, for example, also exhibit UHI effects at smaller spatial scales (e.g. from localized groups of buildings, parking lots, etc.). The UHI modifies local meteorology, exacerbates local air pollution, reduces visibility, impacts agriculture, increases water usage, and exacerbates morbidity during urban heat waves (Hunt *et al.*, 2012). Land features and land-use, including terrain (Sharma and Huang, 2012), streets and buildings, building materials, vegetation, and anthropogenic heat (AH) sources (among many other factors) exert strong controls on UHI effects. Some examples are the proximity to ocean, sea, or lake (Chen *et al.*, 2011b; Salamanca *et al.*, 2011; Sharma *et al.*, 2016), type of vegetation and land-cover (Georgescu *et al.*, 2011; Sharma

*et al.*, 2014, 2016), presence of streets, buildings, parking lots, residential *versus* commercial development, city morphology (e.g. horizontal *vs* vertical structure of buildings), surface albedo (Vahmani and Ban-Weiss, 2016), types of construction materials (Santamouris *et al.*, 2011), and sources of AH [e.g. waste heat from air-conditioning (A/C) (Salamanca *et al.*, 2014), power plants (Zevenhoven and Beyene, 2011), transportation and manufacturing (Sailor, 2011), etc.].

All of the above sources of UHI effects are commonly encountered in the Chicago metropolitan area (CMA), which covers the City of Chicago and its suburbs, making it an ideal case study for examining the performance of physically based simulation models of UHI effects. The CMA is located on a relatively flat terrain, with high-density residential development along the shore of Lake Michigan (Figures 1 and 2(a)). It is the third largest metropolitan area in the United States and the largest in the Great Lakes region (based on US Census Bureau). It covers 12 counties in Illinois, two in Wisconsin, and two in Indiana. The CMA is one of the most populous and heavily urbanized areas of the United States. According to US Census Bureau, 40.6% of the Illinois population lives in Cook County,

\*Correspondence to: A. Sharma, Environmental Change Initiative (ECI), University of Notre Dame; 1400 East Angela Boulevard, Unit 117, South Bend, IN 46617, USA. E-mail: asharma7@nd.edu

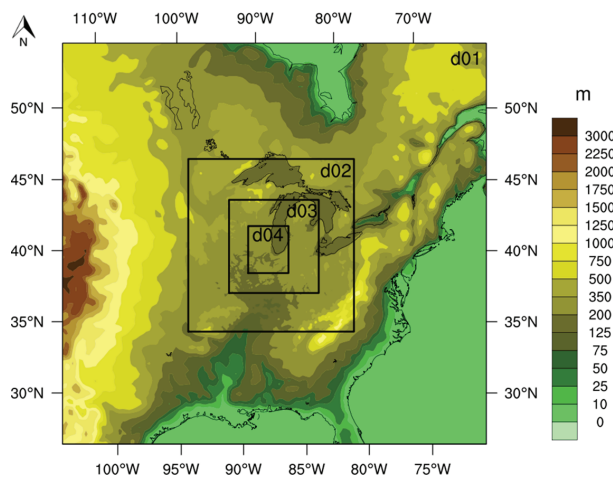


Figure 1. The domain and geographical features of interest to this study with four two-way nested domains for the WRF model with grid size of 27, 9, 3, and 1 km as d01, d02, d03, and d04, respectively, overlaid on a terrain height map. The orientation indicated by north arrow shown here applies to all subsequent figures depicting aerial view. [Colour figure can be viewed at [wileyonlinelibrary.com](http://wileyonlinelibrary.com)].

which contains much of the CMA. The population of Cook County alone ( $\sim 5.2$  million) exceeds the individual population of 29 US states. The total population of the CMA is about 8.6 million. The CMA is a major industrial centre in the United States. The surrounding land is fertile, and has been extensively drained and developed for agriculture. Abundance of flora and fauna provides ecosystem services to local and regional residents. With expansion of suburban communities in recent years, urban areas are growing parallel to the lakeshore and into previously suburban, agricultural, or undeveloped areas.

According to recent estimates from Chicago Metropolitan Agency for Planning (CMAP: <http://www.cmap.illinois.gov/data/land-use/inventory>), over 44% of the land area in the CMA is classified as developed land-use; the rest is either agricultural land or vacant/wetlands/open space. Of the developed land, nearly two-thirds is residential. Land-use characteristics in the CMA are also rapidly changing in some areas. For example, early 245 km $^2$  of land identified as agricultural in 2001 were converted to another use by 2005. Increasing urban and suburban development in the CMA affects the intensity and spatial extent of UHI effects, and poses challenges for energy supply, transportation, ecological conservation, water resource management (water supply and stormwater), agriculture, and human quality of life (Susan, 2007). The rapid conversion of agricultural to urban/residential land calls attention to the need to regularly update land-cover and land-use data sets used in high-resolution mesoscale models. In many modeling studies, however, land-cover data sets have not been kept up to date, and do not accurately reflect the study period (Sertel *et al.*, 2010; Törmä *et al.*, 2015).

Like much of the Midwest region, the CMA experiences large daily and seasonal variations in air temperature. Summers are hot and humid, and winters are cold and windy. In recent decades, a statistically significant warming trend

has been observed over the Midwest [US Global Change Research Program (USGCRP), 2013]. Associated with such warming are increased incidence of heat waves: which we will define as a period of time when maximum temperature is above 32.2 °C (90 °F). Heat waves can have important impacts on human health. For example, the severe heat wave in 1995 in the CMA was responsible for about 750 deaths (Karl and Knight, 1997; Chuang *et al.*, 2013). Elevated night temperatures over multiple days, which are affected by UHI effects, are also implicated in human health impacts of heat waves (Semenza *et al.*, 1996).

Also of meteorological significance is the lake breeze of nearby Lake Michigan, which helps regulate coastal temperatures (Changnon *et al.*, 1996). The effects of the lake breeze on the CMA has been investigated via measurements and numerical modeling in several previous studies (Keeler and Kristovich, 2012; Meir *et al.*, 2013; Conry *et al.*, 2014, 2015). During the afternoon, land areas in the CMA become hot relative to Lake Michigan, creating a high-pressure ridge over the lake and lower pressure due to UHI over the land, causing hot air over the CMA to rise. This vertical transport results in cooler near-surface air flowing from the lake as the lake breeze. Previous studies have shown that the lake breeze in Chicago can penetrate 15–30 km inland, moving cool humid air from Lake Michigan into the city, at times even penetrating to the outer suburbs of the CMA. A stronger lake breeze reduces the UHI, substantially suppressing heating over urban areas, with the most significant impact occurring near the lakeshore (Atkinson, 1989; Laird *et al.*, 2001).

Depending on the specific characteristics of urban areas, with growing urbanization in a warming climate, the urban diurnal temperature range (DTR) ( $T_{\max} - T_{\min}$ ) is likely to decrease more than in rural areas, amplifying the UHI effect (Wang *et al.*, 2012). In general, diurnal extreme temperatures ( $T_{\max}$  and  $T_{\min}$ ) are both rising, but the minimum temperature is rising faster, so the DTR is decreasing, and this decrease is larger in urban areas than in rural areas (Fernando *et al.*, 2012). The amplification of UHI may even lead to local meteorological regime shifts with relatively warmer day- and night-time temperatures than in the past and with deeper but weaker nocturnal boundary layers (Emmanuel and Fernando, 2007; Fernando, 2008).

Notwithstanding the lack of quality observational and simulation data that have limited research progress to date, considerable advances have been made on understanding and modeling of UHI effects (Kalkstein and Davis, 1989; Karl *et al.*, 1995; Kunkel *et al.*, 1996; Kalkstein and Greene, 1997; Palecki *et al.*, 2001; Brazel *et al.*, 2007; Pullen *et al.*, 2008; Grimmond and Athanassiadou, 2009; Basara *et al.*, 2010; Grimmond, 2011; Chen *et al.*, 2012; Best and Grimmond, 2014; Park *et al.*, 2014; Georgescu, 2015). These studies have demonstrated that high-resolution mesoscale models need careful selection of urban parameter values to accurately simulate the effects in each region. Regions in the United States like Houston (Chen *et al.*, 2011b), Baltimore-Washington metropolitan area

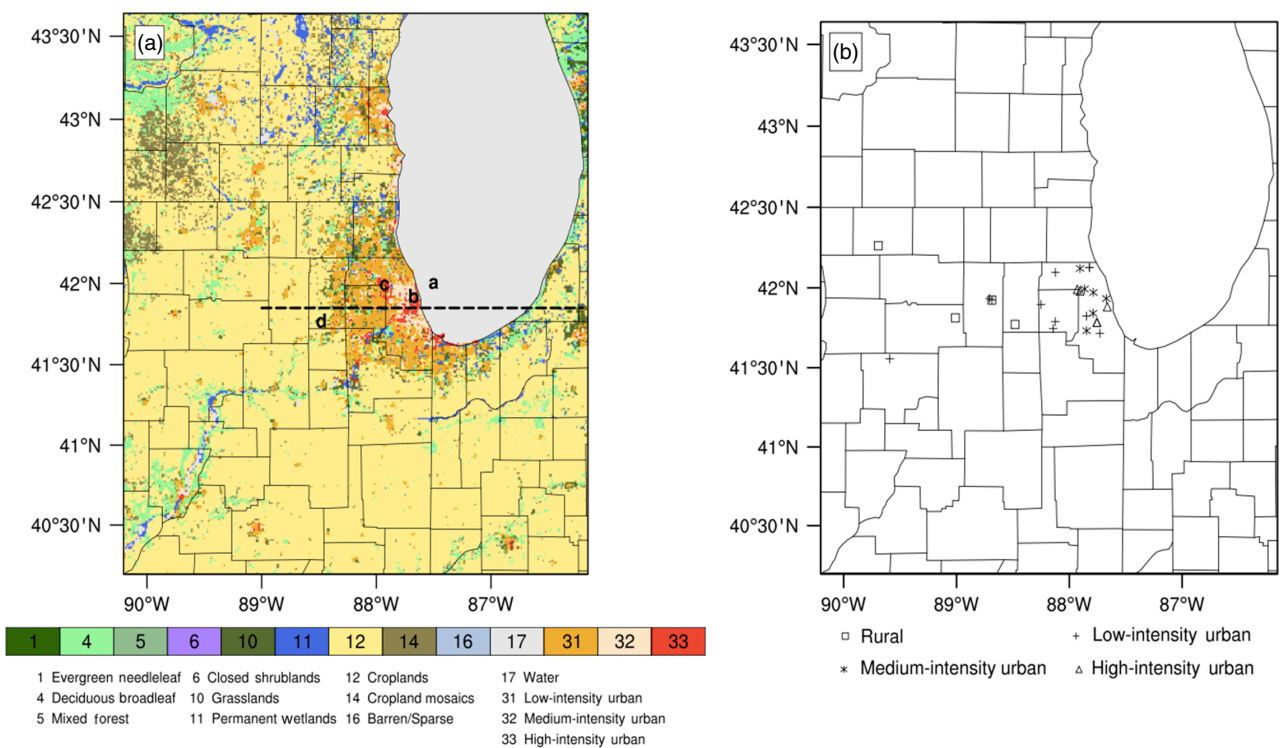


Figure 2. The innermost domain d04 (a) with land-use classification using high-resolution NLCD data. Black dashed line is used for a vertical cross-section analysis for UHI and lake breeze (Figure 9). It also shows different stations used for lake breeze analysis in Figure 10. Here, 'a' refers to the Lake Michigan station; 'b' the station D8777 close to the lakeshore; 'c' the Chicago O'Hare airport; and 'd' the Aurora station; and (b) meteorological stations (Table S1) used to evaluate statistics for different land-use classes. [Colour figure can be viewed at wileyonlinelibrary.com].

(Li *et al.*, 2013a), Phoenix (Grossman-Clarke *et al.*, 2010; Chow *et al.*, 2012; Shaffer *et al.*, 2015), and New York City (Gutiérrez *et al.*, 2015) have already been well studied and urban parameter sets (Wang *et al.*, 2011) have been modified to reflect the unique conditions in each urban centre.

## 2. Experimental design and methods

### 2.1. Synopsis

High-resolution climate modeling using physically based simulation models has not been carried out for the CMA. As noted above, the CMA presents a near ideal case study for evaluating the performance of such models in reproducing UHI effects and the occurrence of lake breeze. This article addresses this opportunity by evaluating the sensitivity of a high-resolution climate model implemented over the CMA and adjoining rural areas shown in Figure 2(a). For our study, we analyse the sensitivity of simulated UHI effects to several important factors: (1) initialization of soil moisture and soil temperature, (2) the spatial resolution of the land-use representation, and (3) the choice of the different urban parameterizations. In addition, we analyzed the complex interaction between land-use, UHI effects, and lake breeze.

### 2.2. WRF implementation

Numerical simulations were performed using the Weather Research and Forecasting (WRF) model, version 3.6

(Skamarock *et al.*, 2005), which is a non-hydrostatic, compressible model. WRF was nested across several domains, and Figure 1 shows details of terrain and the extent of each domain. The model grid was configured so that the outermost domain covers the Laurentian Great Lakes, and the innermost domain covers the CMA and adjoining rural and agricultural areas. The grid spacing (grid points) of these four two-way nested domains were 27 km ( $99 \times 99$ ), 9 km ( $155 \times 166$ ), 3 km ( $190 \times 190$ ), and 1 km ( $319 \times 379$ ), respectively. The model was implemented with 40 pressure-based terrain following vertical levels from the surface to 100 hPa, with the first 17 levels being in the lower 1.5 km and the first model level at 21 m from ground.

Time-varying, large-scale, 3-h National Centers for Environmental Prediction (NCEP) North American Regional Reanalysis (NARR) simulations at 32-km resolution (<http://rda.ucar.edu/datasets/ds608.0/>) were applied as lateral boundary conditions to the outermost domain, with dynamical downscaling to interior domains. Owing to the proximity of the Lake Michigan and the influence of the Great Lakes in the outermost domain (Figure 1(a)), the lake and sea surface temperatures were updated at 3-h intervals using NCEP archives (<ftp://polar.ncep.noaa.gov/pub/history/sst>) to capture the possible lake effects in the WRF model. High-resolution static surface fields, such as terrain height and land-use categories, were also input to the corresponding nested domain boundary conditions. Hourly instantaneous outputs were used to analyse the

UHI and lake breeze sensitivity studies. Henceforth, unless otherwise stated, our discussion refers to the innermost 1-km domain over the CMA. Figure 2(a) shows the land-use categories used in the innermost domain of the WRF model based on 30-m 2006 National Land Cover Data set (NLCD 2006) (Fry *et al.*, 2011) with urbanization over much of the CMA, and adjoining regions covered primarily by agricultural land.

WRF has multiple parameterizations for its physics components: microphysics, convection, radiation, boundary layer, and surface. Previous studies identified the following combination of physical parameterizations over Chicago (Smith and Roebber, 2011; Sharma *et al.*, 2014, 2016; Conry *et al.*, 2015). We utilized a four-layer Noah land surface model (LSM: Chen and Dudhia, 2001). Sub-grid scale cumulus convective parameterization was turned on only for the two outermost domains (27 and 9 km), invoking the Kain-Fritsch scheme (Kain, 2004). We selected WRF single-moment three-class simple ice scheme (WSM3; Hong *et al.*, 2004) for microphysics as it is a sufficiently accurate scheme to model precipitation during this study period. We selected the Dudhia scheme (Dudhia, 1989) for shortwave and the Rapid Radiative Transfer Model for longwave radiation parameterizations (Mlawer *et al.*, 1997). The Monin-Obukhov similarity scheme was used for the surface-layer, and Mellor-Yamada-Janjic scheme (Janjic, 1994) for the planetary boundary layer.

The uWRF setup for studying sensitivities to urban canopy models (UCMs) included (1) a BULK parameterization scheme which represents zero-order effects of urban surfaces to reproduce the resultant urban effect associated with the land-use and vegetation characteristics over urban grid points by means of modified roughness length, surface albedo, heat capacity ( $1.0E6\text{ J m}^{-3}\text{ K}^{-1}$  for roof and building walls and  $1.4E6\text{ J m}^{-3}\text{ K}^{-1}$  for ground), and thermal conductivity ( $0.75\text{ J m}^{-1}\text{ s}^{-1}\text{ K}^{-1}$  for roof and building walls and  $0.4\text{ J m}^{-1}\text{ s}^{-1}\text{ K}^{-1}$  for ground) (Chen and Dudhia, 2001; Liu *et al.*, 2006; Chen *et al.*, 2011a); (2) a single layer urban canopy model (SLUCM) parameterization which uses a two-dimensional street canyon to explicitly parameterize canyon radiative transfer, turbulence, momentum, and heat fluxes. It accounts for different urban surfaces: roof, wall, and road. The SLUCM also has the capabilities of studying the impact of AH fluxes due to A/C, transportation, and human metabolism (Kusaka *et al.*, 2001; Kusaka and Kimura, 2004; Lee *et al.*, 2011); (3) building effect parameterization (BEP) which treats urban surfaces three-dimensionally, and considers heat in the buildings and the effects of vertical and horizontal surfaces on temperature, momentum, and turbulent energy (Martilli *et al.*, 2002); and (4) coupled BEP with a multi-layer building energy model (BEP + BEM) which accounts for energy exchanges happening between the interior of building and the outer atmosphere (Salamanca and Martilli, 2010) for the CMA. The urban parameterization schemes are discussed in Salamanca *et al.* (2011) and the model setup and methods are the same as employed in Sharma *et al.* (2014, 2016). Based on Akbari and Rose (2008), we modified urban parameters for the

uWRF model to reflect current urban conditions in the CMA (Table 1). Estimates of other relevant parameters are obtained from CMAP (<http://www.cmap.illinois.gov>) or were recommended in discussions with the City of Chicago. We used the NLCD 2006 (Fry *et al.*, 2011) to represent the modern-day land-use and land-cover (LULC) within the Noah LSM and National Urban Database and Access Portal Tool (NUDAPT; Ching *et al.*, 2009) data set for the highly urbanized city of Chicago. These data were aggregated to the respective grid resolution of each domain. For SLUCM, we used AH profile averaged over CMA for summers based on empirical estimated values by Sailor and Lu (2004) (Figure S1). SLUCMAH requires that AH be specified as an input, while BEP and BEP + BEM compute AH using a parameterization scheme. The model explicitly accounts for sources of AH (sensible and latent). To account for AH, we treated A/C usage as a primary cause. Therefore, our model has A/C switched on 24 h a day with 75% efficiency. The target indoor temperature is  $25^\circ\text{C}$  with a comfort range of  $0.5^\circ\text{C}$ . The peak heat generated by other equipment in buildings is estimated as  $28\text{ W m}^{-2}$  from 0800 to 1800 LST and  $7\text{ W m}^{-2}$  during night (Note LST = UTC-5).

### 2.3. Sources of observational data

The uWRF simulations were evaluated using multiple Mesowest urban and rural stations located in the innermost domain that provided near-surface meteorological point data (<http://mesowest.utah.edu>). The location and land-use classification of stations are shown in Figure 2(b) and Table S1, and observed 2-m temperatures and 10-m wind speed and direction were used for comparison. Although our mesoscale simulations are high resolution (1-km innermost domain), they are still much coarser than the footprint of *in situ* point measurements, so observations should capture more spatial variability than the model. It is also important to note that point measurements are not fully representative of simulated values for a  $1 \times 1\text{ km}$  grid cell that contains them and classification of observational stations as ‘urban’ or ‘rural’, is at times poor (Stewart and Oke, 2012). This should be kept in mind when considering model evaluation results.

For spatial comparisons, we utilized Moderate Resolution Imaging Spectroradiometer (MODIS) Aqua satellite land surface (skin) temperature observations to compare with the simulations (Leroyer *et al.*, 2011; Zhang *et al.*, 2011; Li *et al.*, 2013b; Hu *et al.*, 2014). The MODIS product used was MYD11A1 version 5, which provides daily level 3 global 1-km pixel grid based observations.

### 2.4. Choice of time-period for the study

Historically, over one-third of the summer and spring days show lake breeze over the CMA (Lyons, 1972; Laird *et al.*, 2001). The period from 16 to 18 August 2013 was relatively hot with no precipitation over the CMA, but with strong lake breeze under quiescent synoptic conditions (Conry *et al.*, 2015; Sharma *et al.*, 2016). We used the criteria developed by Laird *et al.* (2001) to determine the

Table 1. Modified urban parameters for uWRF model used in the study.

Parameters	HI*	MI*	LI*
Urban fraction	0.83	0.82	0.55
Building height (m)	18	15	6
Roof width (m)	22	20	8
Thermal conductivity ( $\text{W m}^{-1} \text{K}^{-1}$ )	0.75	0.75	0.75
Surface albedo of roof	0.2	0.2	0.2
Surface albedo of wall	0.2	0.2	0.2
Surface albedo of ground	0.15	0.15	0.15
Peak number of occupants per unit floor area (persons $\text{m}^{-2}$ )	0.02	0.02	0.02
Scale factor for peak heat generated by equipment ( $\text{W m}^{-2}$ )	28	28	28

\*Land-use urban classes are low, medium, and high intensity as indicated by LI, MI, and HI.

lake-breeze period from observations with which we separated the lake breeze from the synoptic flow by requiring a change (a) wind conditions between morning and afternoon, and (b) a positive temperature gradient between the Lake Michigan and CMA. This case was used to examine the effects of land data assimilation, sub-grid scale land-cover variability, and their influence on the interaction of UHI effects with the lake breeze. Simulations were conducted from 0700 LST on 15 August 2013 to 1900 LST on 18 August 2013, with the first 12 h for spin up and 3 additional days for analysis. In this article, 'daytime' refers to average conditions in the late afternoon from 1400 to 1700 LST and 'nighttime' refers to average conditions in the very early morning before sunrise from 0200 to 0500 LST over the 3-day period.

## 2.5. High-resolution land data assimilation for UHI simulations

A state-of-the-art high-resolution land data assimilation system (HRLDAS v3.6; Chen *et al.*, 2007) was used to initialize state variables of the Noah LSM for our high-resolution experiments (Table 2). HRLDAS is an uncoupled model that is run offline for each nested domain that integrates fine-scale static land characteristics, e.g.: land-use, terrain height, time-averaged vegetation fraction; observed and derived near-surface meteorological variables. To initialize the uWRF model for each nested domain, HRLDAS was spun up for the preceding year (1 August 2012 to 15 August 2013).

## 2.6. Sensitivity to sub-grid scale land-use variability

At 30-m resolution (the scale of high-resolution NLCD data), a 1-km grid cell contains multiple possibilities of different land-use classes, which presents an opportunity to include considerable sub-grid scale variability within a 1-km aggregate land-cover representation. To illustrate the effects of these more sophisticated schemes, we compared a number of possible land-use classes between MODIS\_30 s resolution ( $\sim 900$  m) and NLCD data for our innermost d04 domain. Using MODIS\_30 s grid cells generally resulted in a single land-use classification for each 1-km grid cell. However, with NLCD data, we observed substantial sub-grid land-use variability in most 1-km cells (see Figure 6 and related discussion in Section 3.2). This

variability was low in the core CMA (since most of the region was classified as urbanized), however, for the outer CMA, a typical 1-km grid cell contained seven to eight different land-use classes.

## 2.7. Interaction of lake breeze and urbanization

To study the interaction of UHI with the lake breeze, two sensitivity experiments for SLUCMAH were performed: an experiment with default NLCD land-use classification and another with NLCD urban land-use classification modified to croplands (agricultural). Land surface data assimilation (HRLDAS v3.6) was also incorporated in these model runs.

To measure the extent/penetration of lake breeze, we also compared simulated 10-m wind speed with observations by choosing four stations as shown in Figure 2(a): (1) the first station 'a' is over the Lake Michigan (Figure 10(a)); (2) the second station 'b' D8777 is close to the lakeshore (Figure 10(b)); (3) the third station 'c' is the O'Hare airport station located around 20-km away from the lakeshore (Figure 10(c)); and (4) the fourth station 'd' near Aurora, IL is approximately 60-km inland from the lake (Figure 10(d)).

## 2.8. Sensitivity of different urban parameterizations

We hypothesize that the sensitivities related to the initialization of soil moisture and temperature (with and without HRLDAS) and the details in the land-use representation (mosaic vs dominant category) along with the choice of urban parameterization will help understand and reduce uncertainties in the numerical modeling of near-surface meteorology. Thus, this study performs the sensitivity on different urban parameterizations, viz., BULK, SLUCM with and without AH, BEP and BEP + BEM using 2-m temperature, and 10-m wind speed analysis for the above land-use modeling approaches (Table 2). The analyses were divided into urban and rural categories. Urban stations were further classified into low-intensity, medium-intensity, and high-intensity land-use classes (refer to Tables S2–S5 for statistics on urban land-use classes). Since the UHI effect is most prominent at night, we aggregated the hourly data into 12-h periods for day (0600–1700 LST) and night (1800–0500 LST) for statistics presented in Tables 3 and 4.

Table 2. Design of experiments for different uWRF model sensitivities performed in the study.

Experiment	Land-use	Urban parameterization	Comment
1	NLCD 2006 + NUDAPT	BULK	HRLDAS
<i>Sensitivity with land data assimilation</i>			
2	NLCD 2006 + NUDAPT	SLUCMnoAH	HRLDAS
3	NLCD 2006 + NUDAPT	SLUCMAH	noHRLDAS
4	NLCD 2006 + NUDAPT	SLUCMAH	HRLDAS
5	NLCD 2006 + NUDAPT	BEP + BEM	noHRLDAS
6	NLCD 2006 + NUDAPT	BEP + BEM	HRLDAS
<i>Sensitivity with inclusion of sub-grid land-use variability</i>			
7	NLCD 2006 + NUDAPT	SLUCMAH	HRLDAS + dominant land-use; $N^* = 1$
8	NLCD 2006 + NUDAPT	SLUCMAH	HRLDAS + mosaic land-use; $N^* = 8$
<i>Interaction of lake breeze and urbanization</i>			
9	NLCD 2006 + urban modified to cropland	SLUCMAH	HRLDAS
10	NLCD 2006 + NUDAPT	SLUCMAH	HRLDAS

\*Maximum number of land-use classes considered in a grid cell for the experiment.

### 3. Results

In this section, we discuss the results related to four sensitivity studies outlined in Section 2.1.

#### 3.1. High-resolution land data assimilation for UHI simulations

Figure 3 shows the uWRF model initialization with NARR data for soil moisture and soil temperature. Simulations without HRLDAS (referred to as ‘noHRLDAS’) did not resolve soil moisture from LULC variations, which was almost uniform with  $\sim 0.1 \text{ m}^3 \text{ m}^{-3}$ . HRLDAS on the other hand captured the heterogeneity of soil moisture; soil moisture over urban areas was typically very low ( $0.05 \text{ m}^3 \text{ m}^{-3}$ ) compared to agricultural areas ( $0.25 \text{ m}^3 \text{ m}^{-3}$ ) (Figure 3(a) and (b)). Similarly, heterogeneity was simulated in soil temperature when using HRLDAS. The case of noHRLDAS did not show realistic soil temperature over urban areas, whereas HRLDAS showed physically realistic soil temperatures that were higher over urban areas and lower over agricultural areas (Figure 3(c) and (d)). Findings that are illustrated in Figure 3 are for the top land surface layer (0.1 m below surface layer), and similar patterns were also observed for the lower layers.

Figure 4 presents the model comparison of 2-m air temperatures overlaid by 10-m wind vectors for different permutations of SLUCM urban parameterizations with and without AH and HRLDAS for nighttime and daytime. SLUCMAH with HRLDAS showed higher 2-m air temperatures during nighttime over the agricultural region and lower temperature over the CMA in comparison to the case with noHRLDAS (Figure 4(a)–(c)). High humidity in agricultural areas led to higher nighttime temperatures because water vapour reduces the loss of longwave radiation from the surface to atmosphere (Ruckstuhl *et al.*, 2007). This was consistent with sensitivity experiments with initial soil temperatures and soil moisture (Figure 3). During the daytime, however, the overall temperatures decreased in comparison with the simulation with noHRLDAS (Figure 4(d)–(f)) due to reduction of artificial heating caused by higher soil moisture and lower

soil temperature with HRLDAS. It was also noted that in the noHRLDAS simulations the lake breeze penetrated deep into the urban areas in comparison to HRLDAS simulations, because there was an overall warming over the non-urban domain due to less moisture and higher soil temperature (Figure 4(e)). The sensitivity of AH with HRLDAS showed that AH produced 3 °C nighttime warming over the CMA (Figure 4(a), (g), (i)). During the daytime, the warming due to AH was not substantial, however, as the lake breeze penetrated over the CMA and reduced the impact of AH (Figure 4(d) and (h)). Figure S2 compares CMA-averaged simulated surface fluxes using three different approaches of SLUCM: HRLDAS noAH, HRLDAS + AH, and noHRLDAS + AH. Figure 5 shows the sensitivity of BEP + BEM scheme to HRLDAS. Therein the 2-m temperatures over urban areas were increased during the nighttime and reduced during the daytime with HRLDAS.

#### 3.2. Sensitivity to sub-grid scale land-use variability

This analysis led us to two important and complementary findings. First, at a resolution  $\sim 1 \text{ km}$  and below, the model did not have much sub-grid variability for 30 s resolution data and a dominant land-use approach could be used without any substantial loss of information from the primary data (MODIS). Second, when using NLCD data, there was a large impact of sub-grid scale variability at 1-km resolution (Figure 6), and modeling with the conventional dominant land-use classification approach would frequently lead to a loss of information from the primary land-cover data sets and also potentially spurious results from the uWRF simulations due to misclassification of the land-use in each cell. Thus, accounting influence of multiple land-use classes was appropriate within each grid cell for studying UHI effects study.

To test the sensitivity to land-use categories within a grid cell (Table 2), we compared the traditional approach of using a dominant land-use class for each grid cell (dominant approach) with a new approach using multiple classes to represent the sub-grid variability of the land-cover (mosaic approach) (Li *et al.*, 2013b). Note

Table 3. Statistical comparison of the simulated and observed rural 2-m temperatures ( $^{\circ}\text{C}$ ) and 10-m wind speeds ( $\text{m s}^{-1}$ ) for 16–18 August 2013. The criterion for HR calculation is  $1^{\circ}\text{C}$  for temperature and  $1 \text{ m s}^{-1}$  for wind speed.

Rural stations		2-m temperature ( $^{\circ}\text{C}$ )			10-m wind speed ( $\text{m s}^{-1}$ )		
		MB	RMSE	HR	MB	RMSE	HR
SLUCMnoAH	Day	-2.49	2.78	0.98	0.82	1.73	0.61
	Night	-0.23	1.69	0.76	0.63	1.28	0.64
SLUCMAH*	Day	4.81	5.64	0.13	1.37	2.19	0.49
	Night	-5.65	6.08	0.99	0.97	1.42	0.47
SLUCMAH	Day	-2.18	2.60	0.63	0.71	1.72	0.65
	Night	0.23	2.21	0.65	0.62	1.24	0.66
SLUCMAH + mosaic	Day	0.04	2.13	0.91	0.85	1.73	0.59
	Night	-0.84	1.71	0.84	0.64	1.26	0.60
BULK	Day	-2.13	2.56	0.97	0.75	1.73	0.60
	Night	0.30	1.71	0.68	0.70	1.22	0.64
BEP	Day	-2.13	2.44	0.98	0.61	1.70	0.65
	Night	-0.02	1.63	0.72	0.72	1.30	0.59
BEP + BEM	Day	-2.21	2.54	0.98	0.61	1.70	0.65
	Night	0.04	1.61	0.73	0.73	1.22	0.61

\*Here we do not use HRLDAS. All other cases utilize HRLDAS.

Table 4. Statistical comparison of the simulated and observed urban 2-m temperatures ( $^{\circ}\text{C}$ ) and 10-m wind speeds ( $\text{m s}^{-1}$ ) for 16–18 August 2013. The criterion for HR calculation is  $1^{\circ}\text{C}$  for temperature and  $1 \text{ m s}^{-1}$  for wind speed.

Urban stations		2-m temperature ( $^{\circ}\text{C}$ )			10-m wind speed ( $\text{m s}^{-1}$ )		
		MB	RMSE	HR	MB	RMSE	HR
SLUCMnoAH	Day	-1.33	2.50	0.00	1.56	2.16	0.41
	Night	-2.41	2.81	0.89	0.94	1.41	0.63
SLUCMAH*	Day	1.21	2.41	0.58	2.00	2.45	0.28
	Night	0.33	3.29	0.34	1.43	1.76	0.45
SLUCMAH	Day	-0.02	1.42	0.78	1.90	2.37	0.31
	Night	0.83	1.94	0.55	0.84	1.29	0.67
SLUCMAH + mosaic	Day	1.20	1.99	0.87	1.60	1.94	0.54
	Night	1.60	2.12	0.44	1.13	1.12	0.71
BULK	Day	0.08	1.50	0.77	1.90	1.23	0.67
	Night	1.89	2.36	0.38	1.46	1.84	0.35
BEP	Day	-1.54	2.38	0.91	0.96	1.76	0.54
	Night	-1.25	1.84	0.92	0.49	1.02	0.79
BEP + BEM	Day	-1.30	1.98	0.91	1.02	1.76	0.50
	Night	-0.42	1.41	0.79	0.56	1.06	0.77

\*Here we do not use HRLDAS. All other cases utilize HRLDAS.

that the mosaic approach was used only with SLUCM and the rest of the urban parameterizations employed the dominant approach. In this experiment, eight most prominent land-use classes were used within a grid cell to represent the impact of sub-grid land-use variability, by employing SLUCMAH with HRLDAS parameterization. Figure 7 compares mosaic and dominant approaches, with Figure 7(a) and (b) showing mosaic and dominant nighttime 2-m temperatures, respectively, overlaid by 10-m winds, while Figure 7(c) shows the difference plot. Figure 7(d)–(f) are the same as Figure 7(a)–(c), except for the daytime. The mosaic showed higher (lower) temperatures over the CMA during nighttime (daytime). Use of mosaic approach better captured the spatial sub-grid variability of nighttime temperatures throughout the domain. There was a 2–3  $^{\circ}\text{C}$  increase within the domain as the urban component in rural grids was retained and released heat, except for sub-urban regions, where the mosaic showed a decrease

in temperature as it accounted for lower temperatures for areas with substantial non-urban components (Figure 7(c)). Similarly, the mosaic showed lower temperatures during the daytime. A strong impact on the lake breeze was seen in both the dominant and mosaic (Figure 7(d) and (e)) approaches, resulting in a shift in the UHI ‘hot spot’ 15–30 km inland.

Mosaic simulations were compared with MYD11A1 version 5 MODIS satellite observations at 1330 LST on 16 August 2013. At this time, the satellite passed the CMA with low cloud coverage. All urban areas under the CMA and Milwaukee showed strong UHI in comparison to adjoining rural/agricultural areas with mosaic simulations and satellite observations (Figure 8). The white colour in satellite observations shows no observations. Simulations and satellite observations show similar patterns over both land and water surface.

For urban areas during daytime, the sensible heat flux was lower for the mosaic approach than for the dominant

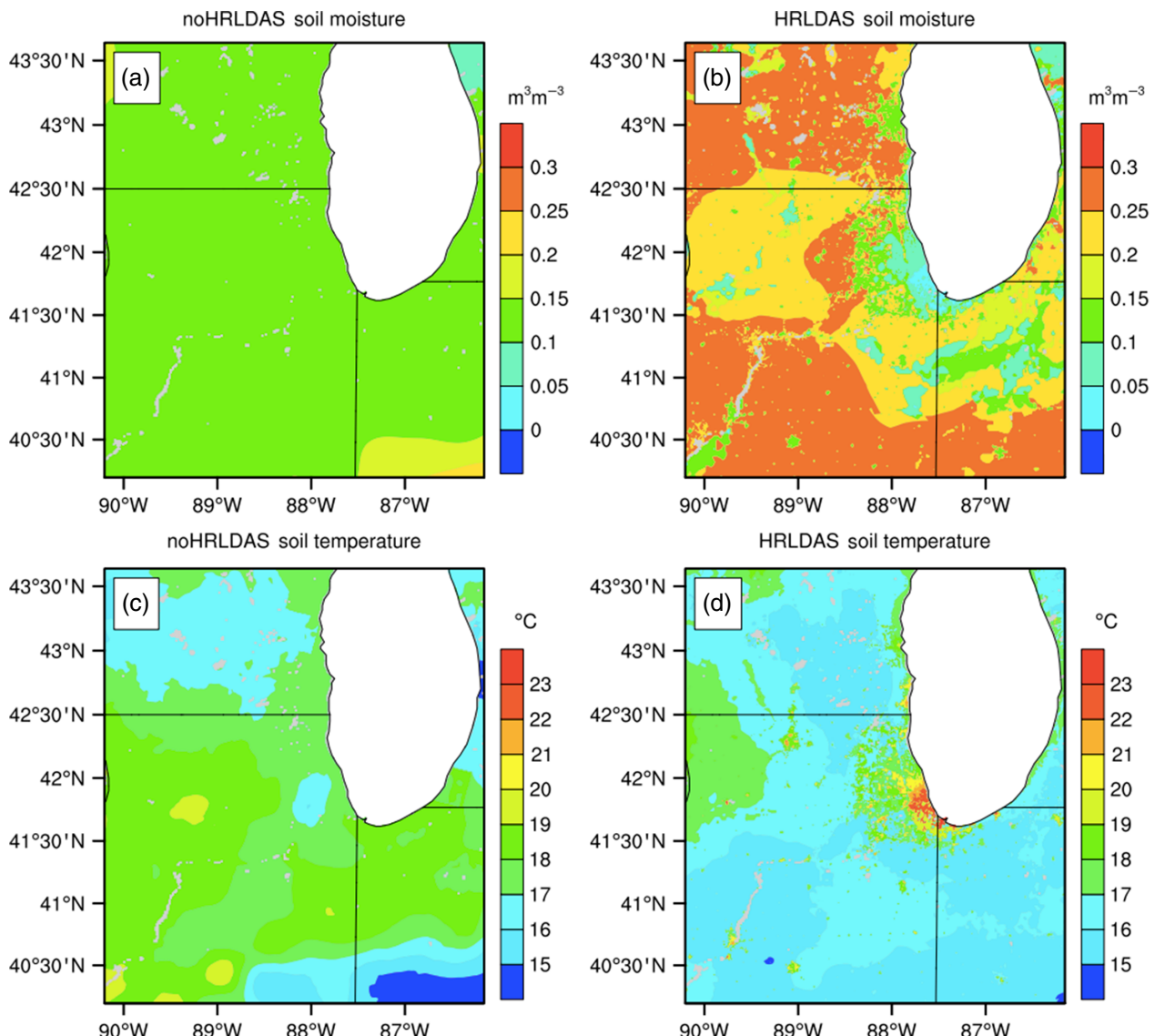


Figure 3. Comparison of WRF model initialization at 0700 LST on 15 August 2013 for (a) soil moisture with noHRLDAS and (b) with HRLDAS; (c) soil temperature with noHRLDAS and (d) with HRLDAS. [Colour figure can be viewed at [wileyonlinelibrary.com](http://wileyonlinelibrary.com)].

approach as mosaic accounted for non-urban land-use component within urban areas that released less sensible and more latent heat flux during daytime in the atmosphere (Figure S3). Latent heat flux was generally lower for urban than rural (Figure S3). In particular, latent heat flux increased with the mosaic approach in urban areas due to better representation of non-urban classes. For detailed discussion on surface energy fluxes using dominant and mosaic approaches, refer to Figure S3.

### 3.3. Interaction of lake breeze and urbanization

Figure 9 shows the vertical cross-section of the temperature overlaid by horizontal wind vectors on 17 August 2013, as depicted in a dashed black line in Figure 2(a). Values in the plots are the water vapour mixing ratios ( $\text{kg kg}^{-1}$ ). During the day (1600 LST), the UHI and lake breeze developed close to the ground (Figure 9(a)). The lake breeze showed relatively high wind velocity over the lake, but the velocity was lower as it advected over the

urban areas due to higher surface friction. During the night (0400 LST), the land surface eventually became cooler than the lake and a land breeze developed (Figure 9(c)). When urban grids were modified to cropland, UHI did not develop and the lake breeze was not as strong as with urbanized grids due to lower temperature (Figure 9(b)). Interestingly, although the lake breeze was weaker with cropland in place, it still penetrated inland as much as in the previous case. One possible explanation is the reduced surface friction of croplands in comparison with urban areas, which results in less reduction in wind velocity with distance in the case of cropland. Therefore, the inland penetration of lake breeze was dependent not only on the temperature difference between lake and land, but also on land-use roughness. As expected, the simulated night temperatures were lower when urban areas were modified to cropland (Figure 9(d)). For both cases, the circulation pattern was observed in the lower atmosphere with positive vertical velocities over urban

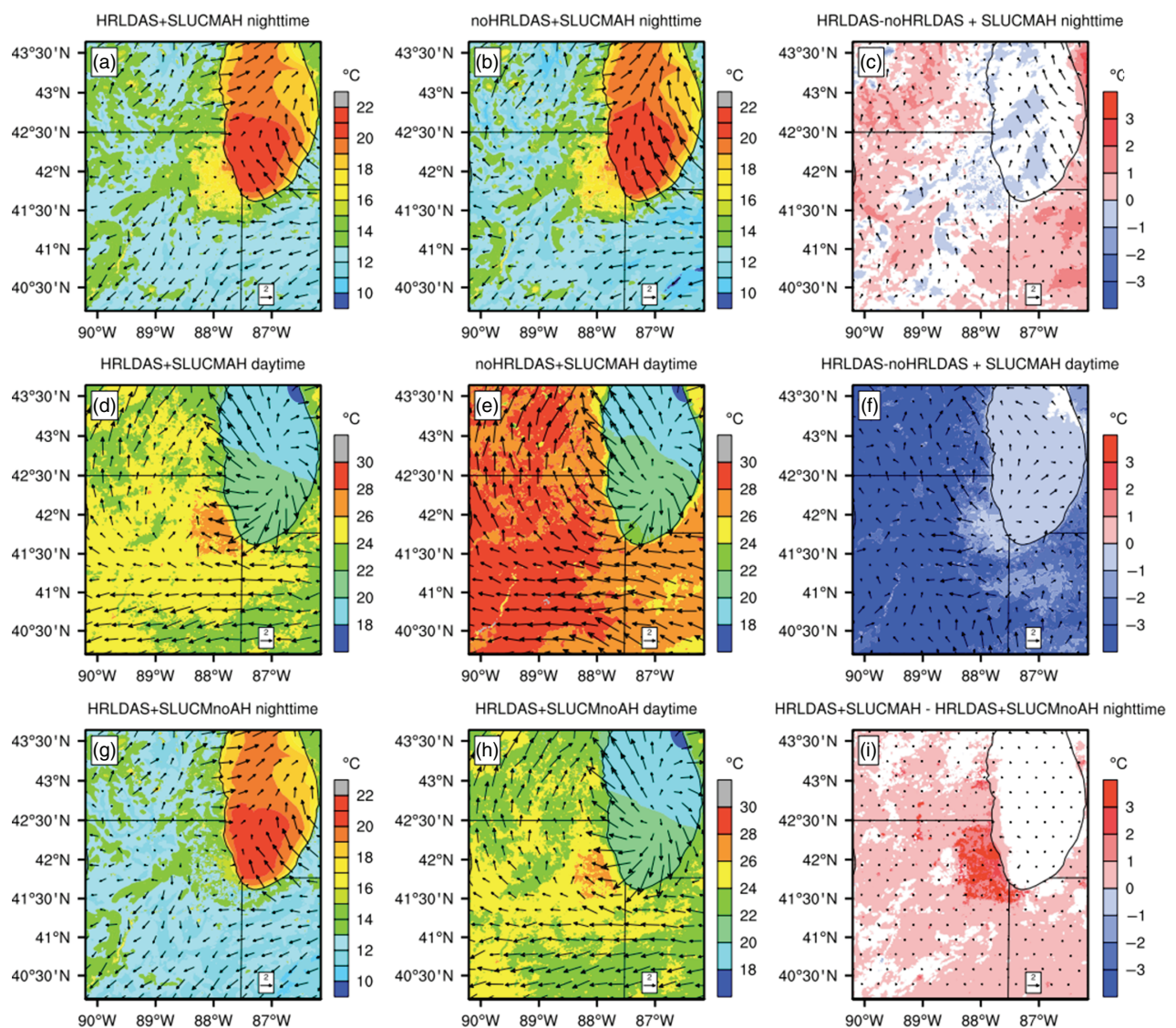


Figure 4. Model comparison of 2-m temperatures overlaid by 10-m wind vectors for nighttime SLUCMAH urban parameterization (a) with HRLDAS; (b) with noHRLDAS; (c) difference plot (a) – (b). Middle panel is same as top panel except that the plots are for daytime. Bottom panel shows the influence of SLUCM without AH (SLUCMnoAH) for nighttime and daytime in (g) and (h), respectively, and (i) nighttime difference between (a) and (g). The white colour in difference plots for panels (c), (f), and (i) refers to a difference  $< 0.2^{\circ}\text{C}$ . The reference wind vectors in each panel figure has units of  $\text{m s}^{-1}$ . [Colour figure can be viewed at wileyonlinelibrary.com].

areas and negative vertical velocities over Lake Michigan (Figure S4).

#### 3.4. Sensitivity of different urban parameterizations

For 10-m winds, in general, the uWRF model showed a mild land breeze (eastward) during the morning on 16 August 2013, and a strong lake breeze (westward) during the afternoon and evenings for all 3 days (Figure 10(a)). This diurnal variation was observed at all distances from the lake. Over land, closest to the lake, the simulated winds were almost as strong as over the lake (Figure 10(b)). However, observations of 10-m wind speeds close to the lake were of poor quality due to disruption of the flow by tall buildings in downtown Chicago. Further from the lake, but still in urban areas, the lake breeze wind speed in simulations and observations decreased due to the surface resistance (Figure 10(c) and (d)). Farthest from the lake

(Figure 10(d)), both simulations and observations began to show a systematic reduction in wind speed, and the local winds also more closely followed the synoptic flow from the large-scale forcing (e.g. Figure 7(d)). For all combinations of land-use and urban parameterizations shown in Table 2, simulated 10-m wind speed directions closely matched observations as shown in Figure 10. The statistics of 10-m wind speeds magnitude for rural and urban stations were all comparable and are shown in Tables 3 and 4, respectively.

The sensitivity of 2-m temperature to different SLUCM parameterizations was minimal for rural stations, except for those close to the CMA that are affected by advection of lake breeze and urban heating. Nevertheless, simulations for 2-m temperature over rural stations showed reduced root mean square error (RMSE) and mean bias (MB), and higher hit rate (HR) with HRLDAS in comparison

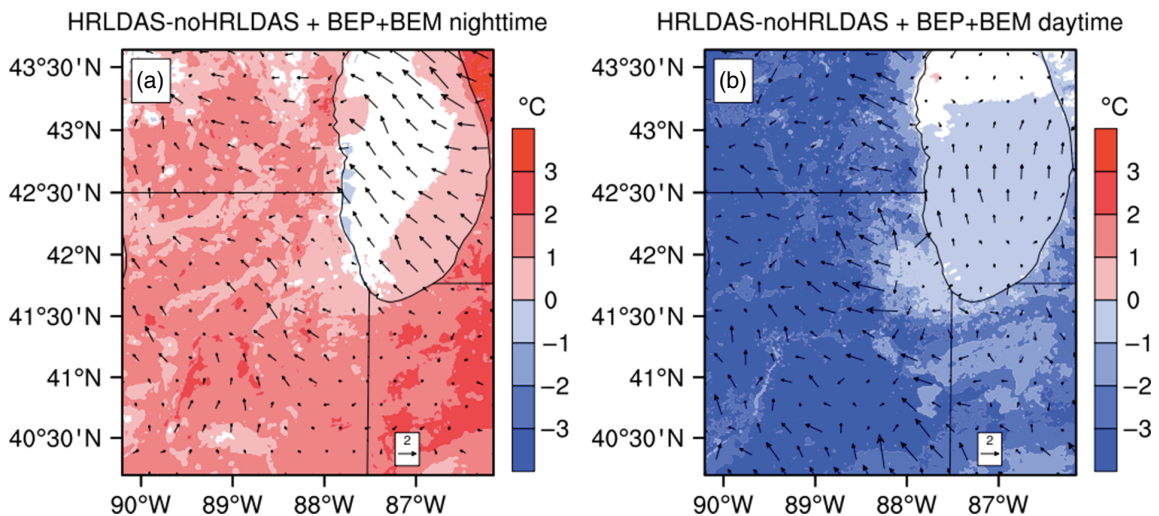


Figure 5. Model comparison for difference between HRLDAS and noHRLDAS of 2-m temperatures overlaid by 10-m wind vectors for BEP + BEM urban parameterization for (a) nighttime and (b) daytime. The white colour means the difference  $<0.2^{\circ}\text{C}$ . The reference wind vectors in each panel figure has units of  $\text{m s}^{-1}$ . [Colour figure can be viewed at [wileyonlinelibrary.com](http://wileyonlinelibrary.com)].

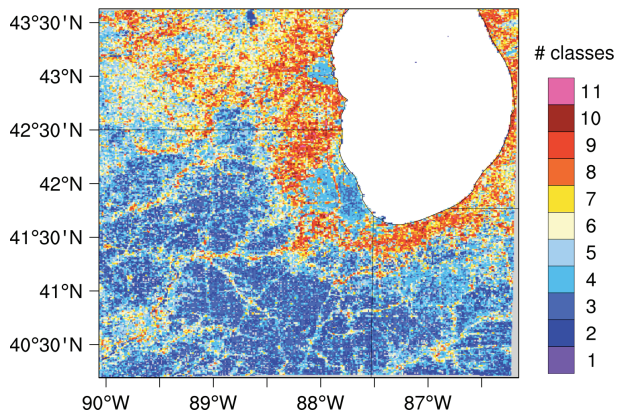


Figure 6. Number of land-use classes in each grid cell ( $1 \times 1 \text{ km}$ ) for innermost domain d04 using NCLD 2006 30 m resolution data. [Colour figure can be viewed at [wileyonlinelibrary.com](http://wileyonlinelibrary.com)].

to the case when HRLDAS was not employed, since soil moisture and soil temperature were well represented after land data assimilation; note that default NARR lacked a robust representation of land surface forcing data (Table 3 and Figure 11(d)). Inclusion of land-use heterogeneity using HRLDAS + SLUCM + mosaic also improved peak day rural 2-m temperatures (Table 3).

In comparison to rural stations, urban stations also showed significant sensitivity to different SLUCM parameterizations. Within different SLUCM parameterizations, the performance of SLUCMs at night improved in cases when AH was included in the model land-use forcing. The night RMSE was lowest with HRLDAS + SLUCMAH (Figure 11 and Table 4). Simulations for SLUCM with no AH showed cold biases (MB) for both during day and night for all urban classes (Table 4 and Tables S2–S4). Simulations with no HRLDAS also showed cold bias during night for all urban classes. HRLDAS + SLUCM + mosaic performed well in comparison with other SLUCM schemes, especially over

low-intensity urban areas as it accounted for the aggregated effects of multiple land-use classes within the suburban areas (Figure 6), which was missing in other SLUCM parameterizations.

Comparing all UCM schemes over urban areas (Figure 12), BEP + BEM with HRLDAS showed lowest MB and RMSE for both during day and night (Table 4) due to explicit accounting of AH from urban structures compared to SLUCMs diurnal climatological AH profile (Figure S1). However, BULK showed least RMSE for high-intensity urban area, even though the parameterization is relatively simplistic. For low-intensity urban areas, BEP showed the least RMSE (a little lower than BEP + BEM). For all urban land-use classes, night MB and RMSE decreased from BEP to BEP + BEM because the BEM within BEP + BEM accounts for latent and sensible AH separately by prescribed A/C usage (Section 2.2; Salamanca and Martilli, 2010) and would lead to higher sensible heat released to the atmosphere to maintain prescribed indoor temperatures within comfort level limits. For all parameterizations, MB and RMSE were typically lower at night and higher at day for both rural and urban stations with different urban classes.

#### 4. Discussions and conclusions

This article evaluates simulations of summertime high temperatures in CMA due to UHI effects, and interaction of UHI with lake breeze from the Lake Michigan. Sensitivity of these simulated phenomena to the urban parameterization schemes employed in the uWRF model was evaluated. All available urban parameterizations in uWRF were evaluated in the experiments: the BULK urban scheme, SLUCM with and without AH, BEP, and BEP + BEM scheme. The study also examined the use of a land surface data assimilation technique (HRLDAS) for potential reduction of uncertainties resulting from initial

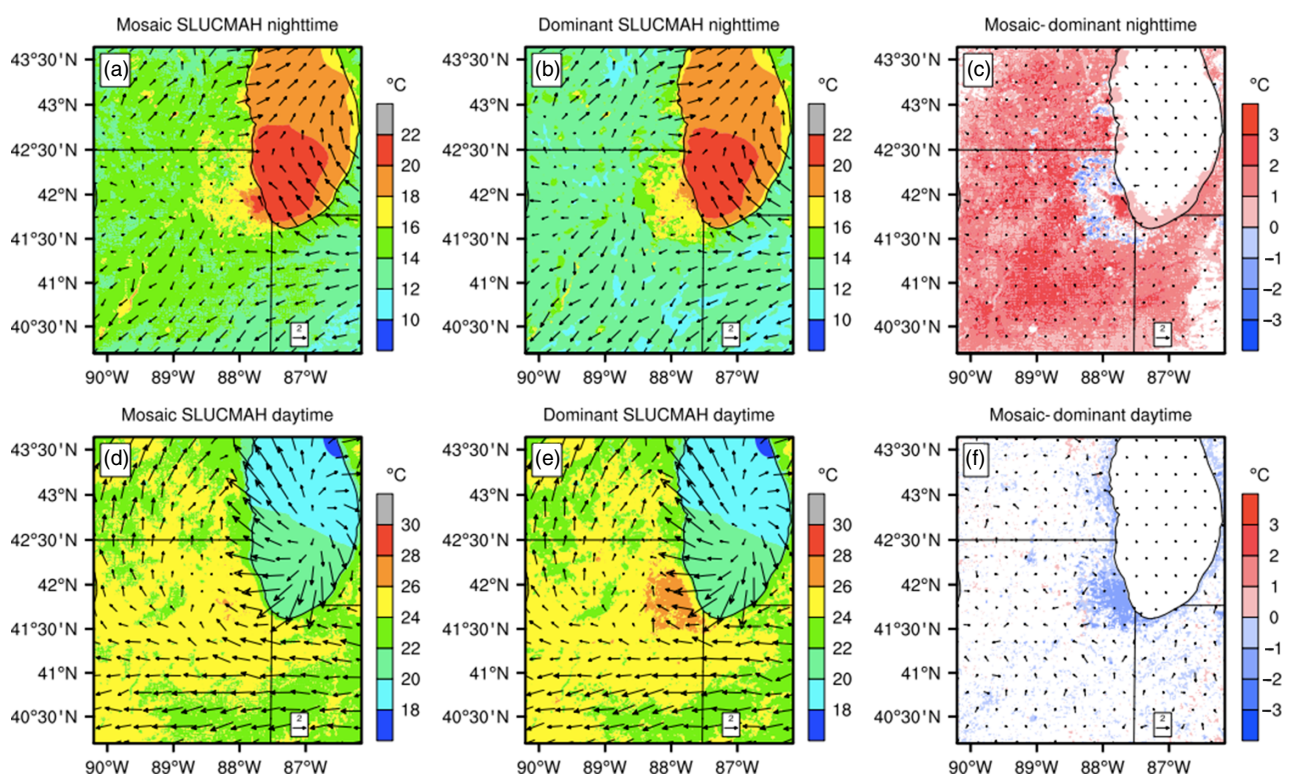


Figure 7. Model comparisons of 2-m temperatures overlaid by 10-m wind vectors for nighttime for SLUCMAH urban parameterization (a) with mosaic land-use approach (eight most prominent classes within a grid cell); (b) dominant land-use approach; and (c) difference plot (a) – (b). Bottom panel is same as top panel except that the plots are for daytime. The white colour in difference plots for panels (c) and (f) refers to a difference  $<0.2^{\circ}\text{C}$ . The reference wind vectors in each panel figure has units of  $\text{m s}^{-1}$ . [Colour figure can be viewed at wileyonlinelibrary.com].

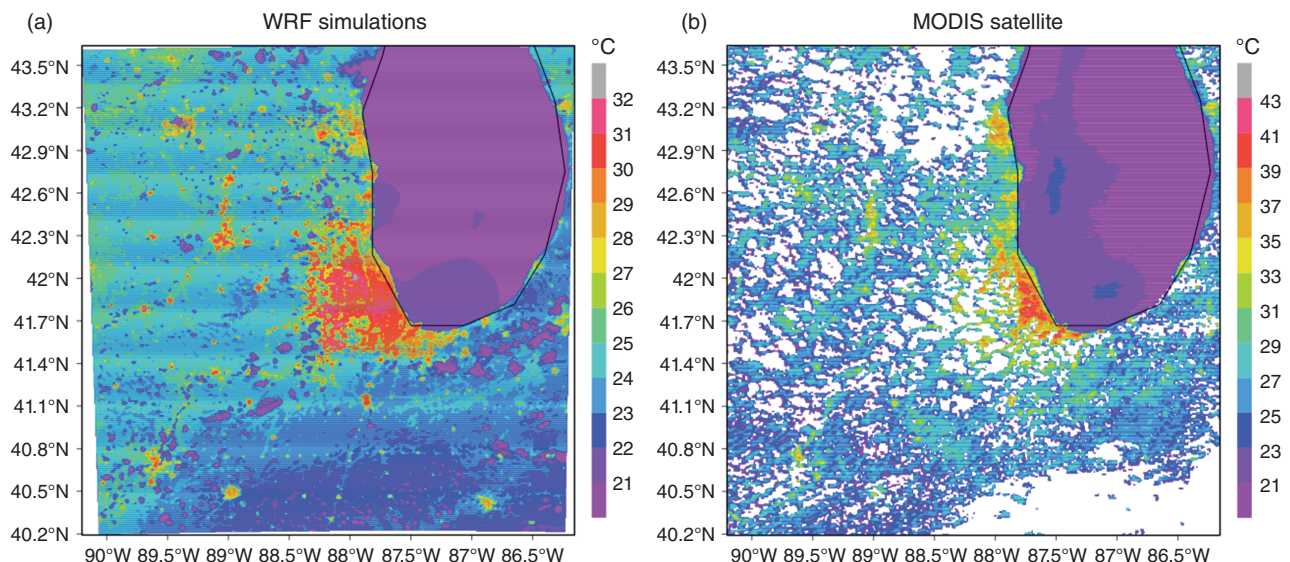


Figure 8. Comparison of (a) surface skin temperatures for SLUCMAH + mosaic with HRLDAS simulations, and (b) radiative land surface temperature from MODIS satellite data at 1330 LST. Note that the colour scale is different for both plots since here the aim is to show the similar spatial signature and not a direct numerical comparison. [Colour figure can be viewed at wileyonlinelibrary.com].

conditions, along with mosaic approach for LSM which accounts for sub-grid variability of land-cover.

In addition to normal UHI effects related to land-cover, the study evaluated simulations of more complicated urban phenomena where UHI effects due to land-cover interact with the lake breeze from Lake Michigan. The

simulations showed that the lake breeze likely penetrates about 15–30 km inland over the CMA and then fades away upon interacting with the synoptic flow. The influence of UHI effects during the daytime was reduced by lake breeze along the highly urbanized CMA coastline. Simulations of urban land-use modified to cropland showed

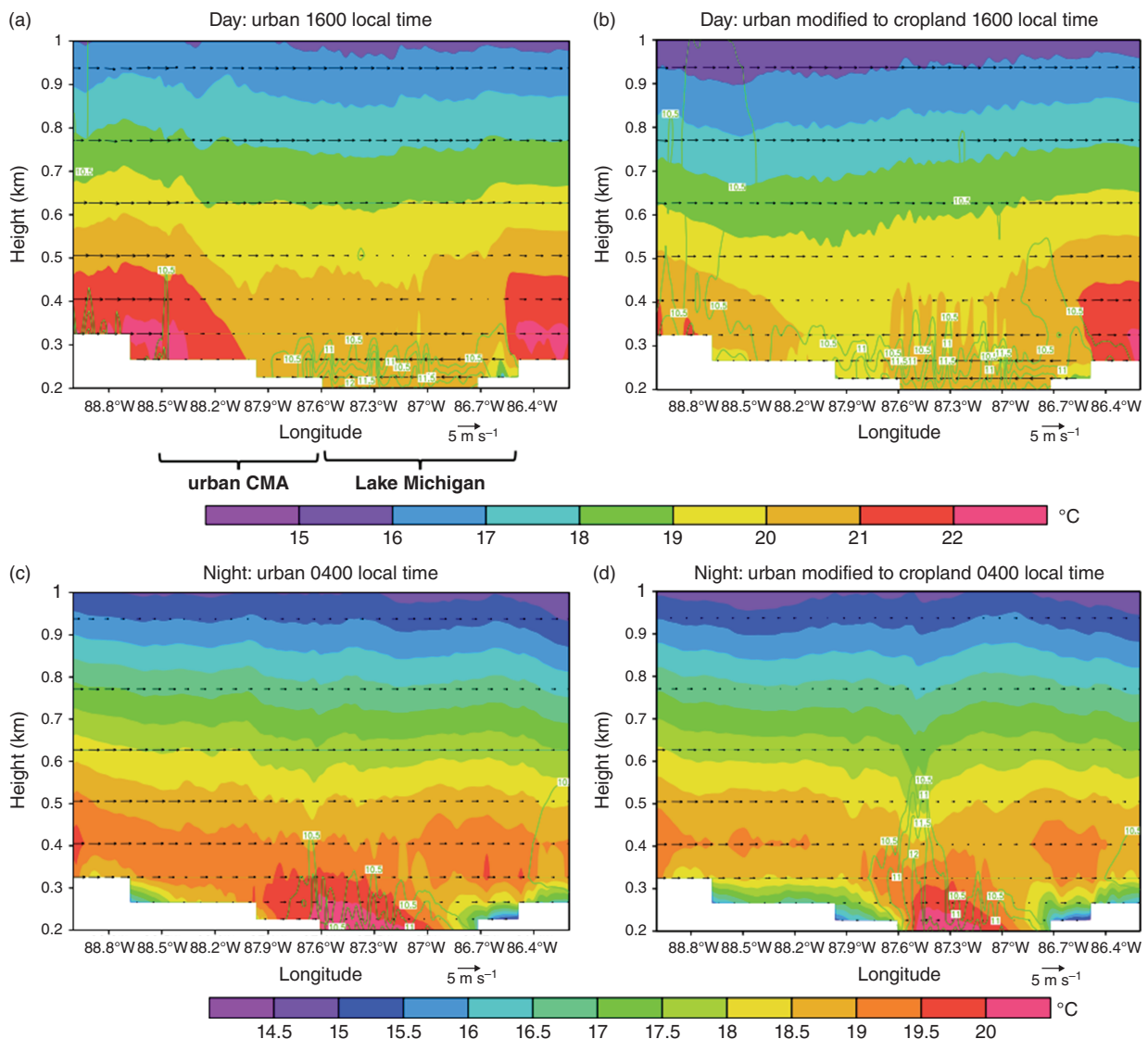


Figure 9. Vertical cross-section of the CMA (as shown in Figure 2(a) as a black dashed line) with contoured temperature ( $^{\circ}\text{C}$ ) and horizontal wind speed vectors on 17 August 2013 showing a schematic of lake breeze phenomenon for SLUCMAH with HRLDAS (a) during day (1600 LST) for default urbanization, (b) with hypothetical situation when urban areas are modified to croplands. Panels (c) and (d) are same as (a) and (b) respectively except for night (0400 LST). Values in the plots are the water vapour mixing ratios ( $\text{kg kg}^{-1}$ ). [Colour figure can be viewed at [wileyonlinelibrary.com](http://wileyonlinelibrary.com)].

reduced temperatures but an unabated lake breeze with strength almost similar to the case with urban land-use. In the cropland case, the temperature difference was low between urban areas modified to cropland and surrounding cropland/rural areas, so was surface friction on land, with one counteracting the other in determining the lake breeze.

Initial conditions were found to be an important source of model bias. The inclusion of land surface data assimilation using HRLDAS significantly changed both soil moisture and soil temperature initialization, which in turn modified the simulation of 2-m air temperature and 10-m wind speed. Note, there were no quantitative comparisons against observations of soil moisture and soil temperature, only qualitative discussion about anticipated outcomes on near-surface temperatures and wind speeds with different land-covers in contrast to NARR initialization were

performed. Urban schemes that used the mosaic approach better captured the spatial variability of temperature, particularly at night. These effects were particularly pronounced in the Chicago suburbs where noticeable surface LULC variability within respective grid cells was common. In absence of strong synoptic flow, with improved initial conditions and improved land surface modeling techniques, the more complicated urban schemes performed better. Urban schemes that used the mosaic approach did not necessarily achieve the best performance in comparison with other schemes in terms of reproducing point observations, but the ability to resolve sub-grid spatial variability in suburban areas was an important advantage of this approach.

With inclusion of appropriate and realistic parameter values for the CMA for all available urban schemes, we have attempted to reduce the bias in the uWRF

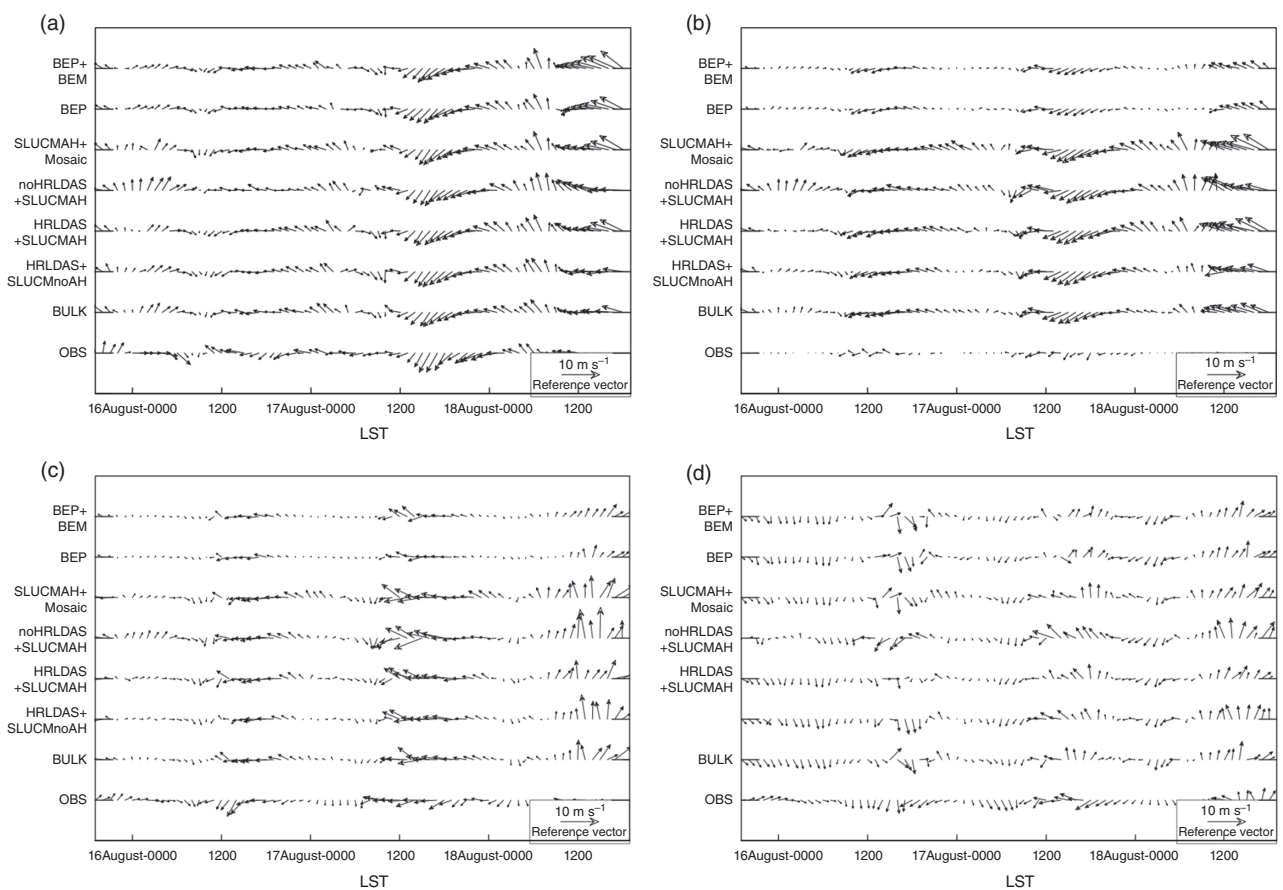


Figure 10. 10-m winds ( $\text{m s}^{-1}$ ) for different urban parameterizations and land-use at (a) Lake Michigan; (b) D8777, a station close to the lake; (c) O'Hare airport; and (d) Aurora. Also, see Figure 2(a) for location of these stations. Reference vector ( $\text{m s}^{-1}$ ) in panel plots shows eastward wind direction (from CMA to the Lake Michigan).

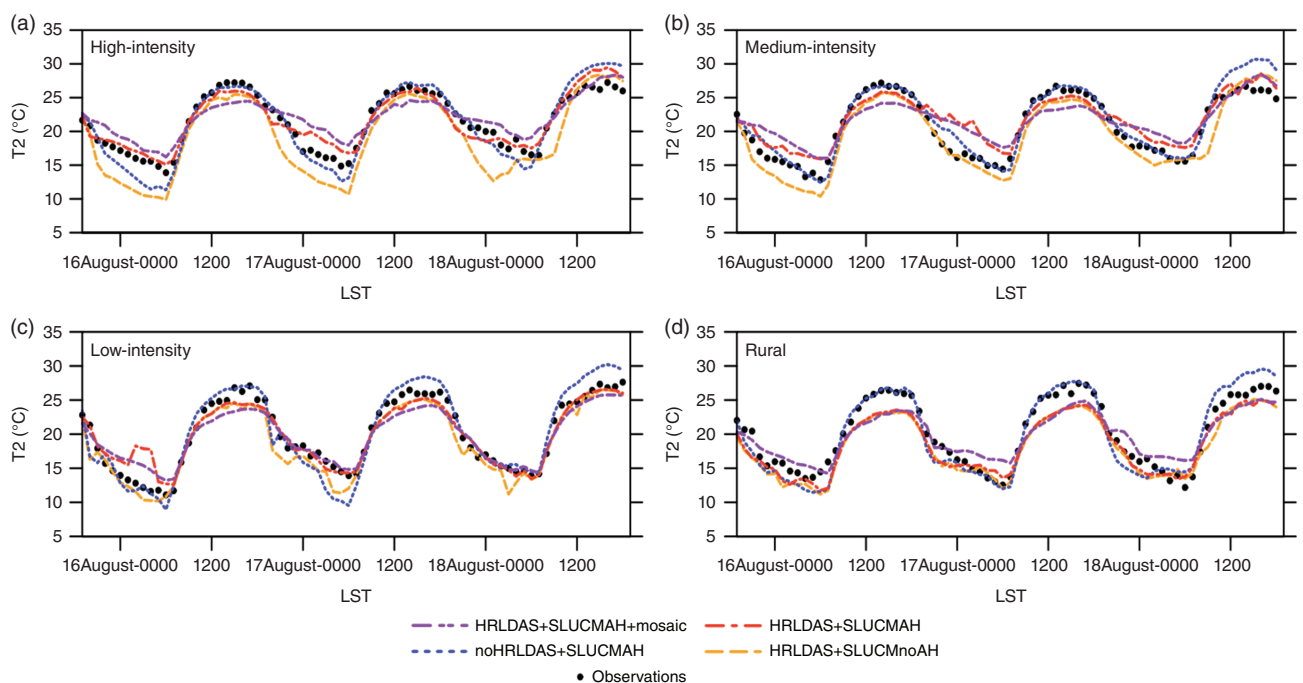


Figure 11. 2-m temperatures ( $^{\circ}\text{C}$ ) for different SLUCM parameterizations and for different urban (high intensity, medium intensity, and low intensity) and rural LULC classes. The stations with latitude–longitude and LULC information are shown in Table S1. [Colour figure can be viewed at wileyonlinelibrary.com].

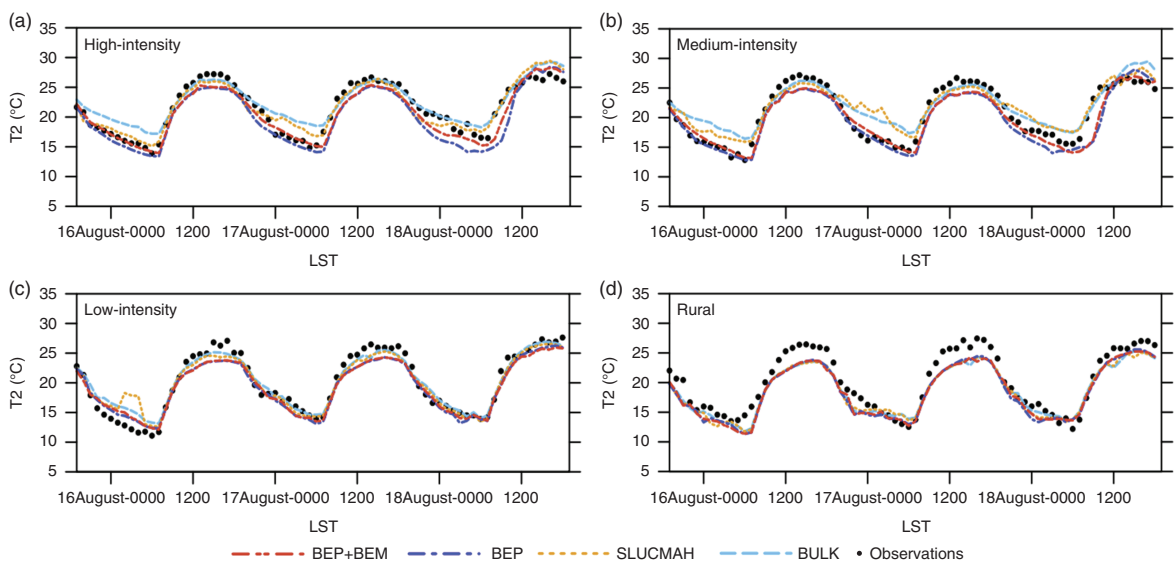


Figure 12. 2-m temperatures ( $^{\circ}\text{C}$ ) for different UCM parameterizations using HRLDAS and for different urban (high intensity, medium intensity, and low intensity) and rural LULC classes. The stations with latitude–longitude and LULC information are shown in Table S1. [Colour figure can be viewed at [wileyonlinelibrary.com](http://wileyonlinelibrary.com)].

simulations as much as possible without artificially tuning parameters for each urban scheme to match the observations. We hope the methodology can be of use in guiding future urban studies, especially in view of the fact that the approaches used here can readily be applied to other urban areas, including coastal cities whose UHI effects are influenced by the marine environment. We also discussed the strengths of a mosaic approach to account for sub-grid land-use variability, which will be valuable in future studies if high-resolution land-use maps are available for other parts of the world. Overall, this article is a step forward in understanding and modeling the physics of urban environments using different urban simulation schemes combined with urban parameters customized for individual cities. It is our hope that improvements in modelling UHI effects will help predict the impacts of climate variability and climate change on cities and help develop appropriate adaptation/mitigation strategies to heat-related impacts.

## Acknowledgements

The research work is supported by National Science Foundation (NSF) grant number: AGS 0934592, USDA-NIFA Agriculture and Food Research Initiative (awards 2015-67003-23508 and 2015-67003-23460), the Notre Dame Environmental Change Initiative, the Center for Sustainable Energy, and the City of Chicago. Simulations were performed with NCAR Yellowstone and the NCSA Blue Waters GLCPC computing grants for supercomputing facilities and the Center for Research Computing at the University of Notre Dame. Authors also acknowledge Dr. Dan Li for help with sub-grid scale land-use variability implementation and Zachariah Silver for processing raw station data sets.

## Appendix: List of acronyms

A/C	Air-conditioning
AH	Anthropogenic heat
BEM	Building energy model
BEP	Building effect parameterization
BEP + BEM	Building effect parameterization + multi-layer building energy model
CMA	Chicago metropolitan area
CMAP	Chicago Metropolitan Agency for Planning
DTR	Diurnal temperature range
HI	High intensity
HR	Hit rate
HRLDAS	High-resolution land data assimilation system
LI	Low intensity
LSM	Land surface model
LST	Local standard time
LULC	Land-use/land-cover
MB	Mean bias
MI	Medium intensity
MODIS	Moderate Resolution Imaging Spectroradiometer
MYD11A1	MODIS/Aqua LST/E L3 global 1 km grid
NARR	North American Regional Reanalysis
NCEP	National Centers for Environmental Prediction
NLCD	National Land Cover Data
noHRLDAS	Without high-resolution land data assimilation system
NUDAPT	National Urban Database and Access Portal Tool
RMSE	Root mean square error
SLUCM	Single layer urban canopy model
SLUCMAH	Single layer urban canopy model with anthropogenic heat
SLUCMnoAH	Single layer urban canopy model with no anthropogenic heat
UCM	Urban canopy model
UHI	Urban heat island
UTC	Coordinated universal time
USGCRP	US Global Change Research Programme
WRF	Weather Research and Forecasting model

## Supporting information

The following supporting information is available as part of the online article:

**Figure S1.** Anthropogenic heat (AH) profiles for the Chicago metropolitan area (CMA): (a) average winter and summer profiles. Winter profile is higher than summer due to exacerbated building heating in extreme cold weather; and (b) AH profiles for summers for different urban land-use classifications.

**Figure S2.** Comparison of CMA-averaged energy budget fluxes for different combinations of SLUCM with and without AH, and with and without HRLDAS.

**Figure S3.** Comparison of domain averaged energy budget fluxes for dominant and mosaic parameterizations for rural and urban areas. Urban component of mosaic/dominant refers to the sub-grid relative contribution of the urban fraction within each grid cell for respective approaches.

**Figure S4.** Vertical cross-section of the CMA on 17 August 2013 at 1600 LST for SLUCM during daytime showing contours of (a) horizontal wind component and (b) vertical wind component.

**Table S1.** Detailed meteorological station information and their type of MODIS LULC classification used in the study.

**Table S2.** Statistical comparison of simulated and observed 2-m temperatures ( $^{\circ}\text{C}$ ) and 10-m wind speeds ( $\text{m s}^{-1}$ ) for the high-intensity urban stations for 16–18 August 2013. The criterion for hit rate calculation is  $1^{\circ}\text{C}$  for temperature and  $1 \text{ m s}^{-1}$  for wind speed.

**Table S3.** Statistical comparison of simulated and observed 2-m temperatures ( $^{\circ}\text{C}$ ) and 10-m wind speeds ( $\text{m s}^{-1}$ ) for the medium-intensity urban stations for 16–18 August 2013. The criterion for hit rate calculation is  $1^{\circ}\text{C}$  for temperature and  $1 \text{ m s}^{-1}$  for wind speed.

**Table S4.** Statistical comparison of simulated and observed 2-m temperatures ( $^{\circ}\text{C}$ ) and 10-m wind speeds ( $\text{m s}^{-1}$ ) for the low-intensity urban stations for 16–18 August 2013. The criterion for hit rate calculation is  $1^{\circ}\text{C}$  for temperature and  $1 \text{ m s}^{-1}$  for wind speed.

## References

- Akbari H, Rose LS. 2008. Urban surfaces and heat island mitigation potentials. *J. Hum. Environ. Syst.* **11**: 85–101.
- Atkinson BW. 1989. *Meso-Scale Atmospheric Circulations*. Academic Press: San Diego, CA, 495 pp.
- Basara JB, Basara HG, Illston BG, Crawford KC. 2010. The impact of the urban heat island during an intense heat wave in Oklahoma City. *Adv. Meteorol.* **2010**: 230365, doi: 10.1155/2010/230365.
- Best MJ, Grimmond CSB. 2014. Importance of initial state and atmospheric conditions for urban land surface models' performance. *Urban Clim.* **10**: 387–406.
- Brazel A, Gober P, Lee SJ, Grossman-Clarke S, Zehnder J, Hedquist B, Comparri E. 2007. Determinants of changes in the regional urban heat island in metropolitan Phoenix (Arizona, USA) between 1990 and 2004. *Clim. Res.* **33**(2): 171.
- Changnon SA, Kunkel KE, Reinke BC. 1996. Impacts and responses to the 1995 heat wave: a call to action. *Bull. Am. Meteorol. Soc.* **77**(7): 1497–1506.
- Chen F, Dudhia J. 2001. Coupling an advanced land surface-hydrology model with the Penn State-NCAR MM5 modeling system. Part I: model implementation and sensitivity. *Mon. Weather Rev.* **129**(4): 569–585.
- Chen F, Manning KW, LeMone MA, Trier SB, Alfieri JG, Roberts R, Blanken PD. 2007. Description and evaluation of the characteristics of the NCAR high-resolution land data assimilation system. *J. Appl. Meteorol. Climatol.* **46**(6): 694–713.
- Chen F, Kusaka H, Bornstein R, Ching J, Grimmond CSB, Grossman-Clarke S, Zhang C. 2011a. The integrated WRF/urban modelling system: development, evaluation, and applications to urban environmental problems. *Int. J. Climatol.* **31**: 273–288.
- Chen F, Miao S, Tewari M, Bao J-W, Kusaka H. 2011b. A numerical study of interactions between surface forcing and sea breeze circulations and their effects on stagnation in the greater Houston area. *J. Geophys. Res. Atmos.* **116**(D12): D12105, doi: 10.1029/2010JD015533.
- Chen F, Bornstein R, Grimmond S, Li J, Liang X, Martilli A, Miao S, Voogt J, Wang Y. 2012. Research priorities in observing and modeling urban weather and climate. *Bull. Am. Meteorol. Soc.* **93**(11): 1725–1728.
- Ching J, Brown M, McPherson T, Burian S, Chen F, Cionco R, Williams D. 2009. National urban database and access portal tool. *Bull. Am. Meteorol. Soc.* **90**(8): 1157–1168.
- Chow WT, Brennan D, Brazel AJ. 2012. Urban heat island research in Phoenix, Arizona: theoretical contributions and policy applications. *Bull. Am. Meteorol. Soc.* **93**(4): 517–530.
- Chuang WC, Gober P, Chow WT, Golden J. 2013. Sensitivity to heat: a comparative study of Phoenix, Arizona and Chicago, Illinois (2003–2006). *Urban Clim.* **5**: 1–18.
- Conry P, Sharma A, Fernando HJS, Leo LS, Potosnak M, Hellmann J. 2014. Multi-scale simulations of climate-change influence on Chicago heat island, FEDSM2014 Paper No. 21581. In *Proceedings of the Fourth Joint US-European Fluids Engineering Division Summer Meeting*, Chicago, IL, American Society of Mechanical Engineers, FEDSM2014-21581.
- Conry P, Sharma A, Potosnak MJ, Leo LS, Bensman E, Hellmann JJ, Fernando HJ. 2015. Chicago's heat island and climate change: bridging the scales via dynamical downscaling. *J. Appl. Meteorol. Climatol.* **54**(7): 1430–1448, doi: 10.1175/JAMC-D-14-0241.1.
- Dudhia J. 1989. Numerical study of convection observed during the winter monsoon experiment using a mesoscale two-dimensional model. *J. Atmos. Sci.* **46**(20): 3077–3107.
- Emmanuel R, Fernando HJS. 2007. Urban heat islands in humid and arid climates: role of urban form and thermal properties in Colombo, Sri Lanka and Phoenix, USA. *Clim. Res.* **34**: 241–251.
- Fernando HJS. 2008. Polimetrics: the quantitative study of urban systems (and its applications to atmospheric and hydro environments). *Environ. Fluid Mech.* **8**(5–6): 397–409.
- Fernando HJS, Dimitrova R, Sentic S. 2012. Urban environments meet climate change. In *Human Health and National Security Implications of Climate Change*, Fernando HJS, Klaic Z, McCulley JL (eds). Springer: Netherlands, doi: 10.1007/978-94-007-2430-3; ISBN 978-94-007-2429-7.
- Fry J, Xian G, Jin S, Dewitz J, Homer C, Yang L, Barnes C, Herold N, Wickham J. 2011. Completion of the 2006 national land cover database update for the conterminous United States. *Photogramm. Eng. Remote Sens.* **77**(9): 858–864.
- Georgescu M. 2015. Challenges associated with adaptation to future urban expansion. *J. Clim.* **28**(7): 2544–2563.
- Georgescu M, Lobell DB, Field CB. 2011. Direct climate effects of perennial bioenergy crops in the United States. *Proc. Natl. Acad. Sci. USA* **108**(11): 4307–4312.
- Grimmond CSB. 2011. Climate of cities. In *Routledge Handbook of Urban Ecology*, Douglas I, Goode D, Houck M, Wang R (eds). Routledge: London and New York, NY, 103–119.
- Grimmond CSB, Athanassiadou M. 2009. In *Meteorological and Air Quality Models for Urban Areas*, Baklanov A (ed) (vol. 140). Springer: Heidelberg, Germany.
- Grossman-Clarke S, Zehnder JA, Loridan T, Grimmond CSB. 2010. Contribution of land use changes to near-surface air temperatures during recent summer extreme heat events in the Phoenix metropolitan area. *J. Appl. Meteorol. Climatol.* **49**(8): 1649–1664.
- Gutiérrez E, González JE, Martilli A, Bornstein R, Arend M. 2015. Simulations of a heat-wave event in New York City using a multilayer urban parameterization. *J. Appl. Meteorol. Climatol.* **54**(2): 283–301.
- Hong SY, Dudhia J, Chen SH. 2004. A revised approach to ice microphysical processes for the bulk parameterization of clouds and precipitation. *Mon. Weather Rev.* **132**(1): 103–120.
- Hu L, Brunsell NA, Monaghan AJ, Barlage M, Wilhelmi OV. 2014. How can we use MODIS land surface temperature to validate long-term urban model simulations? *J. Geophys. Res. Atmos.* **119**(6): 3185–3201.

- Hunt JC, Timoshkina YV, Bohnenstengel SI, Belcher S. 2012. Implications of climate change for expanding cities worldwide. *Proc. ICE Urban Des. Plan.* **166**(4): 241–254, doi: 10.1680/udap.10.00062.
- Janic ZI. 1994. The step-mountain eta coordinate model: further developments of the convection, viscous sublayer, and turbulence closure schemes. *Mon. Weather Rev.* **122**(5): 927–945.
- Kain JS. 2004. The Kain-Fritsch convective parameterization: an update. *J. Appl. Meteorol. Climatol.* **43**(1): 170–181.
- Kalkstein LS, Davis RE. 1989. Weather and human mortality: an evaluation of demographic and interregional responses in the United States. *Ann. Assoc. Am. Geogr.* **79**(1): 44–64.
- Kalkstein LS, Greene JS. 1997. An evaluation of climate/mortality relationships in large US cities and the possible impacts of a climate change. *Environ. Health Perspect.* **105**(1): 84.
- Karl TR, Knight RW. 1997. The 1995 Chicago heat wave: how likely is a recurrence? *Bull. Am. Meteorol. Soc.* **78**(6): 1107–1119.
- Karl TR, Knight RW, Plummer N. 1995. Trends in high-frequency climate variability in the twentieth century. *Nature* **377**: 217–220.
- Keeler JM, Kristovich DAR. 2012. Observations of urban heat island influence on lake-breeze frontal movement. *J. Appl. Meteorol. Climatol.* **51**(4): 702–710.
- Kunkel KE, Changnon SA, Reinke BC, Arritt RW. 1996. The July 1995 heat wave in the Midwest: a climatic perspective and critical weather factors. *Bull. Am. Meteorol. Soc.* **77**(7): 1507–1518.
- Kusaka H, Kimura F. 2004. Coupling a single-layer urban canopy model with a simple atmospheric model: impact on urban heat island simulation for an idealized case. *J. Meteorol. Soc. Jpn.* **82**(1): 67–80.
- Kusaka H, Kondo H, Kikegawa Y, Kimura F. 2001. A simple single-layer urban canopy model for atmospheric models: comparison with multi-layer and slab models. *Bound.-Layer Meteorol.* **101**(3): 329–358.
- Laird NF, Kristovich DA, Liang XZ, Arritt RW, Labas K. 2001. Lake Michigan lake breezes: climatology, local forcing, and synoptic environment. *J. Appl. Meteorol. Climatol.* **40**(3): 409–424.
- Lee SH, Kim SW, Angevine WM, Bianco L, McKeen SA, Senff CJ, Trainer M, Tucker SC, Zamora RJ. 2011. Evaluation of urban surface parameterizations in the WRF model using measurements during the Texas Air Quality Study 2006 field campaign. *Atmos. Chem. Phys.* **11**(5): 2127–2143.
- Leroyer S, Bélair S, Mailhot J, Strachan IB. 2011. Microscale numerical prediction over Montreal with the Canadian external urban modeling system. *J. Appl. Meteorol. Climatol.* **50**(12): 2410–2428.
- Li D, Bou-Zeid E, Baeck ML, Jessup S, Smith JA. 2013a. Modeling land surface processes and heavy rainfall in urban environments: sensitivity to urban surface representations. *J. Hydrometeorol.* **14**(4): 1098–1118.
- Li D, Bou-Zeid E, Barlage M, Chen F, Smith JA. 2013b. Development and evaluation of a mosaic approach in the WRF-Noah framework. *J. Geophys. Res. Atmos.* **118**(21): 11918.
- Liu Y, Chen F, Warner T, Basara J. 2006. Verification of a mesoscale data-assimilation and forecasting system for the Oklahoma City area during the Joint Urban 2003 field project. *J. Appl. Meteorol. Climatol.* **45**(7): 912–929.
- Lyons WA. 1972. The climatology and prediction of the Chicago lake breeze. *J. Appl. Meteorol. Climatol.* **11**(8): 1259–1270.
- Martilli A, Clappier A, Rotach MW. 2002. An urban surface exchange parameterisation for mesoscale models. *Bound.-Layer Meteorol.* **104**(2): 261–304.
- Meir T, Orton PM, Pullen J, Holt T, Thompson WT, Arend MF. 2013. Forecasting the New York City urban heat island and sea breeze during extreme heat events. *Weather Forecast.* **28**(6): 1460–1477.
- Mlawer EJ, Taubman SJ, Brown PD, Iacono MJ, Clough SA. 1997. Radiative transfer for inhomogeneous atmospheres: RRTM, a validated correlated-k model for the longwave. *J. Geophys. Res. Atmos.* **102**(D14): 16663–16682.
- Palecki MA, Changnon SA, Kunkel KE. 2001. The nature and impacts of the July 1995 heat wave in the midwestern United States: learning from the lessons of 1995. *Bull. Am. Meteorol. Soc.* **82**(7): 1353–1367.
- Park SY, Fernando HJS, Yoon SC. 2014. Simulation of flow and turbulence in the Phoenix area using a modified urbanized mesoscale model. *Meteorol. Appl.* **21**: 948–962. doi: 10.1002/met.1442.
- Pullen J, Ching J, Sailor D, Thompson W, Bornstein B, Koracin D. 2008. Progress toward meeting the challenges of our coastal urban future. *Bull. Am. Meteorol. Soc.* **89**(11): 1727–1731.
- Ruckstuhl C, Philipona R, Morland J, Ohmura A. 2007. Observed relationship between surface specific humidity, integrated water vapor, and longwave downward radiation at different altitudes. *J. Geophys. Res. Atmos.* **112**(D3): D03302, doi: 10.1029/2006JD007850.
- Sailor DJ. 2011. A review of methods for estimating anthropogenic heat and moisture emissions in the urban environment. *Int. J. Climatol.* **31**(2): 189–199.
- Sailor DJ, Lu L. 2004. A top-down methodology for developing diurnal and seasonal anthropogenic heating profiles for urban areas. *Atmos. Environ.* **38**(17): 2737–2748.
- Salamanca F, Martilli A. 2010. A new building energy model coupled with an urban canopy parameterization for urban climate simulations – Part II. Validation with one dimension off-line simulations. *Theor. Appl. Climatol.* **99**: 345–356.
- Salamanca F, Martilli A, Tewari M, Chen F. 2011. A study of the urban boundary layer using different urban parameterizations and high-resolution urban canopy parameters with WRF. *J. Appl. Meteorol. Climatol.* **50**(5): 1107–1128.
- Salamanca F, Georgescu M, Mahalov A, Moustaoui M, Wang M. 2014. Anthropogenic heating of the urban environment due to air conditioning. *J. Geophys. Res. Atmos.* **119**(10): 5949–5965.
- Santamouris M, Synnefa A, Karlessi T. 2011. Using advanced cool materials in the urban built environment to mitigate heat islands and improve thermal comfort conditions. *Sol. Energy* **85**(12): 3085–3102.
- Semenza JC, Rubin CH, Falter KH, Selanikio JD, Flanders WD, Howe HL, Wilhelm JL. 1996. Heat-related deaths during the July 1995 heat wave in Chicago. *N. Engl. J. Med.* **335**(2): 84–90.
- Sertel E, Robock A, Ormeci C. 2010. Impacts of land cover data quality on regional climate simulations. *Int. J. Climatol.* **30**(13): 1942–1953.
- Shaffer SR, Chow WTL, Georgescu M, Hyde P, Jenerette GD, Mahalov A, Moustaoui M, Ruddell BL. 2015. Multiscale modeling and evaluation of urban surface energy balance in the phoenix metropolitan area. *J. Appl. Meteorol. Climatol.* **54**(2): 322–338.
- Sharma A, Huang HP. 2012. Regional climate simulation for Arizona: impact of resolution on precipitation. *Adv. Meteorol.* **2012**: 505726, doi: 10.1155/2012/505726.
- Sharma A, Fernando HJ, Hellmann J, Chen F. 2014. Sensitivity of WRF model to urban parameterizations, with applications to Chicago metropolitan urban heat island. In *ASME 2014 Fourth Joint US-European Fluids Engineering Division Summer Meeting*, American Society of Mechanical Engineers, V01DT28A002.
- Sharma A, Conry P, Fernando HJS, Hamlet AF, Hellmann JJ, Chen F. 2016. Green and cool roofs to combat urban heating in Chicago: evaluation with WRF regional climate model. *Environ. Res. Lett.* **11**: 064004, doi: 10.1088/1748-9326/11/6/064004.
- Skamarock WC, Klemp JB, Dudhia J, Gill DO, Barker DM, Wang W, Powers JG. 2005. A description of the advanced research WRF version 2. No. NCAR/TN-468+STR, Mesoscale and Microscale Meteorology Division, National Center for Atmospheric Research, Boulder, CO.
- Smith KR, Roebber PJ. 2011. Green roof mitigation potential for a proxy future climate scenario in Chicago, Illinois. *J. Appl. Meteorol. Climatol.* **50**(3): 507–522.
- Stewart ID, Oke TR. 2012. Local climate zones for urban temperature studies. *Bull. Am. Meteorol. Soc.* **93**(12): 1879–1900.
- Susan S (ed). 2007. Climate change 2007 – the physical science basis: working group I contribution to the fourth assessment report of the IPCC (vol. 4). Cambridge University Press.
- Törmä M, Markkanen T, Hatunen S, Härmä P, Mattila OP, Arslan AN. 2015. Assessment of land-cover data for land-surface modelling in regional climate studies. *Boreal Environ. Res.* **20**(2): 243–260.
- US Global Change Research Program (USGCRP) 2013. Climate assessment report; third assessment.
- Vahmani P, Ban-Weiss G. 2016. Impact of remotely sensed albedo and vegetation fraction on simulation of urban climate in WRF-UCM: a case study of the urban heat island in Los Angeles. *J. Geophys. Res.* **121**: 1511–1531.
- Wang ZH, Bou-Zeid E, Au SK, Smith JA. 2011. Analyzing the sensitivity of WRF's single-layer urban canopy model to parameter uncertainty using advanced Monte Carlo simulation. *J. Appl. Meteorol. Climatol.* **50**(9): 1795–1814.
- Wang K, Ye H, Chen F, Xiong Y, Wang C. 2012. Urbanization effect on the diurnal temperature range: different roles under solar dimming and brightening. *J. Clim.* **25**(3): 1022–1027.
- Zevenhoven R, Beyene A. 2011. The relative contribution of waste heat from power plants to global warming. *Energy* **36**(6): 3754–3762.
- Zhang DL, Shou YX, Dickerson RR, Chen F. 2011. Impact of upstream urbanization on the urban heat island effects along the Washington-Baltimore corridor. *J. Appl. Meteorol. Climatol.* **50**(10): 2012–2029.